

Silver coordination networks and cages based on a semi-rigid bis(isoxazolyl) ligand†

Andrew D. Burrows,^{*a} David J. Kelly,^a Mary F. Mahon,^a Paul R. Raithby,^a Christopher Richardson^{a,b} and Anna J. Stevenson^a

Received 7th January 2011, Accepted 7th March 2011

DOI: 10.1039/c1dt10029g

The semi-rigid ligand 1,4-bis((3,5-dimethylisoxazol-4-yl)methyl)benzene (bisox) reacts with a range of silver(I) salts to give products in which the anions dictate the structure. The reactions with AgNO₃ and AgO₂CCF₃ both lead to compounds in which the anions are coordinated to the silver centres. Thus, the structure of [Ag₂(NO₃)₂(bisox)] **1** contains helical silver-nitrate chains that are linked into sheets by bridging bisox ligands, whereas the structures of [Ag(O₂CCF₃)(bisox)]·0.5X (**2a**, X = MeOH; **2b**, X = MeCN) consist of sheets in which Ag₂(μ-O₂CCF₃)₂ dimers act as 4-connecting nodes. In these structures bisox adopts the S-conformation, with the nitrogen donor atoms *anti* to each other. The reactions of bisox with AgClO₄ and AgBF₄ in methanol give the compounds [Ag₂(bisox)₃]X₂ (**3**, X = ClO₄; **5**, X = BF₄), the structures of which contain triply-interpenetrated sheets with Borromean links and ligands in the S-conformation. Recrystallisation of these compounds from acetonitrile–diethyl ether gives [Ag₂(bisox)₃]X₂·xEt₂O (**4**, X = ClO₄, x = 1; **6**, X = BF₄, x = 1.2). The structures of **4** and **6** contain similar triply-interpenetrated sheets to those in **3** and **5**, though these are sandwiched between sheets of discrete Ag₂(bisox)₃ cages, in which the bisox ligands are in the C-conformation, with the nitrogen donor atoms *syn* to each other. Diethyl ether molecules project through the faces of the cages and template cage formation. Both **4** and **6** lose diethyl ether on heating in vacuum, and convert into **3** and **5**, respectively. This solid state transformation requires a change in conformation of half the bisox ligands, with conversion of **6** into **5** occurring more readily than conversion of **4** into **3**. The reactions of bisox with AgPF₆ and AgSbF₆ in methanol give mixtures of products from which [Ag(bisox)₂]X·0.5bisox (**7**, X = PF₆; **8**, X = SbF₆) can be isolated. Both **7** and **8** have structures containing one-dimensional chains, in which the bisox ligands adopt C-conformations and interconnect distorted tetrahedral silver centres in a pairwise manner generating macrocycles. Additional uncoordinated bisox molecules lie within half of these macrocyclic rings. Recrystallisation of the crude AgSbF₆/bisox reaction mixture from acetonitrile–diethyl ether gives [Ag(bisox)₂]SbF₆ **9**, the structure of which consists of a triply-interpenetrated flattened diamondoid network. A similar structure was observed for [Ag(bisox)₂]CF₃SO₃ **10**, which is formed from the reaction of AgO₃SCF₃ and bisox in methanol.

Introduction

Coordination network structures in which bridging ligands link metal centres or aggregates into extended structures are currently attracting considerable attention.¹ Much of this interest has arisen because these materials, often referred to as metal–organic frameworks, frequently retain their structures and crystallinity on removal of solvents, which enables them to display interesting

porosity properties. Potential applications in gas storage are especially topical,² but porous coordination networks are also attractive for a range of other applications including separations,³ catalysis⁴ and drug delivery.⁵

While rigid ligands are often used to generate inflexible frameworks, there is an increasing recognition that including a degree of flexibility into a network can allow it to reversibly respond to the presence or absence of a guest.⁶ One way of achieving this is to introduce flexibility into a bridging ligand. If the ligand is completely flexible, then it is likely that it would be able to adjust its conformation in a network to produce a non-porous structure. In contrast, use of semi-rigid ligands,⁷ which contain only a limited degree of flexibility, form an attractive strategy towards porous but non-rigid frameworks.

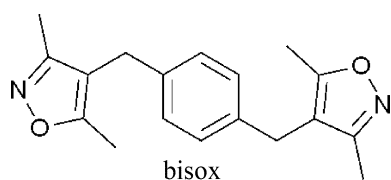
^aDepartment of Chemistry, University of Bath, Claverton Down, Bath, BA2 7AY, UK

^bSchool of Chemistry, University of Wollongong, Northfields Avenue, Wollongong NSW, 2522, Australia

† CCDC reference numbers 804679–804686. For crystallographic data in CIF or other electronic format see DOI: 10.1039/c1dt10029g

Networks formed by silver(I) and ditopic nitrogen donor ligands have attracted interest for a number of reasons.⁸ The $4d^{10}$ silver(I) centre can adopt coordination numbers from 2 to 6, with no strong energetic preference for any particular geometry. A wide range of silver(I) salts are readily available, which makes it relatively straightforward to assess the effects of the counter-ion on the structure of the network formed between the metal and a given ligand.^{9,10} In addition, weak $d^{10} \cdots d^{10}$ interactions can also have a structurally defining effect.

In this paper, we report our studies into the silver(I) networks formed by the semi-rigid bis(isoxazolyl) ligand 1,4-bis((3,5-dimethylisoxazol-4-yl)methyl)benzene, **bisox**. We have previously communicated the results with AgClO_4 .¹¹



The bisox ligand contains methylene spacers between the isoxazole rings and the central benzene ring, allowing it to adopt several conformations. Of these, molecular mechanics suggests the lowest energy conformation is of C_i symmetry, with the nitrogen donor atoms oriented away from each other. For ease of visualization, we denote this the S-conformation. A rotation of 180° about one of the benzene-methylene C–C bonds generates a conformation of C_h symmetry, which we denote the C-conformation. The S- and C-conformations are shown in Fig. 1. While other conformations are also possible by rotation about the $C(\text{sp}^3)$ – $C(\text{sp}^2)$ bonds, the presence of the central benzene ring and two isoxazole rings limit the ligand flexibility.

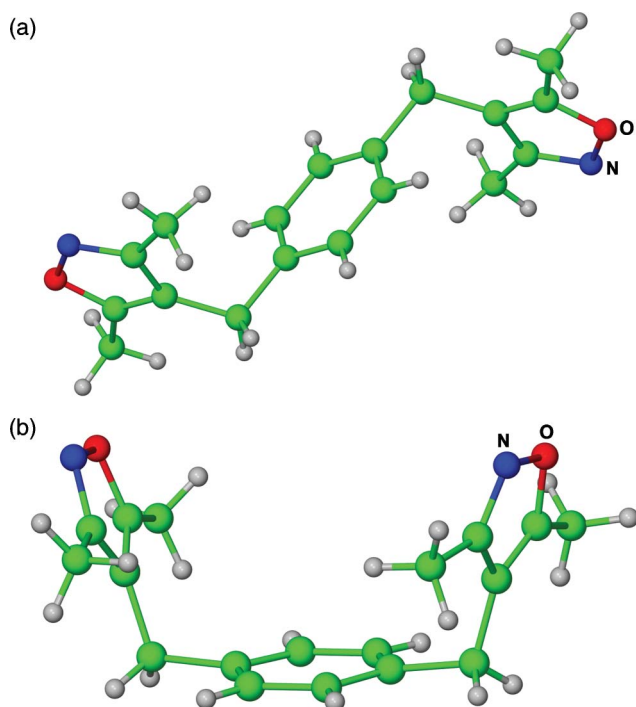


Fig. 1 (a) The S-conformation and (b) the C-conformation for bisox.

Imidazolyl and triazolyl¹² ligands with a similar geometry to bisox have been studied previously. Most notably, the reactions between silver(I) and the bis(pyrazolylmethyl)benzene ligands 1,4-bis(imidazol-1-ylmethyl)benzene (bisim) and 1,4-bis(2-methylimidazol-1-ylmethyl)benzene (bismim) have attracted attention, with examples of polyrotaxanes,¹³ coordination networks^{14,15} and macrocycles¹⁶ illustrating the potential afforded by semi-rigid ligands.

The work reported in this paper represents, to the best of our knowledge, the first use of a bis(isoxazolyl) ligand in forming coordination networks. However, there have been a few examples of networks formed from substituted isoxazole ligands. Silver(I) coordination polymers have been prepared using isoxazolyl ligands containing either amido or sulfide groups,¹⁷ and a copper(II) network has been formed from isoxazole-4-carboxylate.¹⁸

The bisox ligand was prepared by the reaction of 3,3'-(1,4-phenylenebis(methylene))bis(4-hydroxypent-3-en-2-one)¹⁹ with hydroxylamine, and characterised by a combination of NMR spectroscopy, mass spectrometry and microanalysis. In order to keep the number of variables to a minimum, the reactions between bisox and silver(I) salts were carried out in methanol, and slow evaporation of the solvent was used to facilitate crystal growth. The resultant solids were also recrystallised from acetonitrile–diethyl ether.

Reaction of silver(I) nitrate with bisox

The reaction between bisox and silver(I) nitrate in methanol gave crystals that were too small for single crystal analysis. When this compound was recrystallised from acetonitrile–diethyl ether, crystals of $[\text{Ag}_2(\text{NO}_3)_2(\text{bisox})]$ **1** that were suitable for a single crystal X-ray analysis resulted, though the powder X-ray diffraction pattern suggests an unidentified impurity is also present.

The asymmetric unit of **1** contains a silver(I) centre, a coordinated nitrate anion and half of a bisox ligand, with the remainder of this ligand generated by inversion symmetry. Thus, the bisox ligand adopts an S-conformation in this structure. Each silver(I) centre has a distorted trigonal planar geometry, coordinated to two oxygen atoms from different nitrate ions and one nitrogen atom from a bisox ligand. The bond angles around the silver centre range from $101.16(10)^\circ$ to $137.42(10)^\circ$ and the sum of the angles is 355.5° . The nitrate ions bridge between silver(I) centres in the μ - $\kappa^1 O, \kappa^1 O'$ -coordination mode to form helical chains. These chains are cross-linked by the bridging bisox ligands to form two-dimensional sheets, as shown in Fig. 2a. There are two sets of these parallel sheets in the crystal structure, with an angle of 57° between the least squares planes of each set. Similar silver-nitrate chains have been previously observed with 3,6-bis(2-pyrazinyl)-1,2,4,5-tetrazine and 1,4-bis(2-pyridylaminomethyl)benzene co-ligands.²⁰

Each sheet contains 44-membered metallomacrocylic rings which, because of the ligand conformation, adopt 'hour-glass' shapes. Two bisox ligands from the other set of sheets are directed through each of the rings in an example of 2D inclined interpenetration, as shown in Fig. 2b. The isoxazole rings of the interpenetrating ligands lie equidistant between pairs of isoxazole rings in the same metallomacrocylic ring, and distances between the isoxazole planes of 3.3–3.8 Å suggest the presence of $\pi \cdots \pi$ interactions.

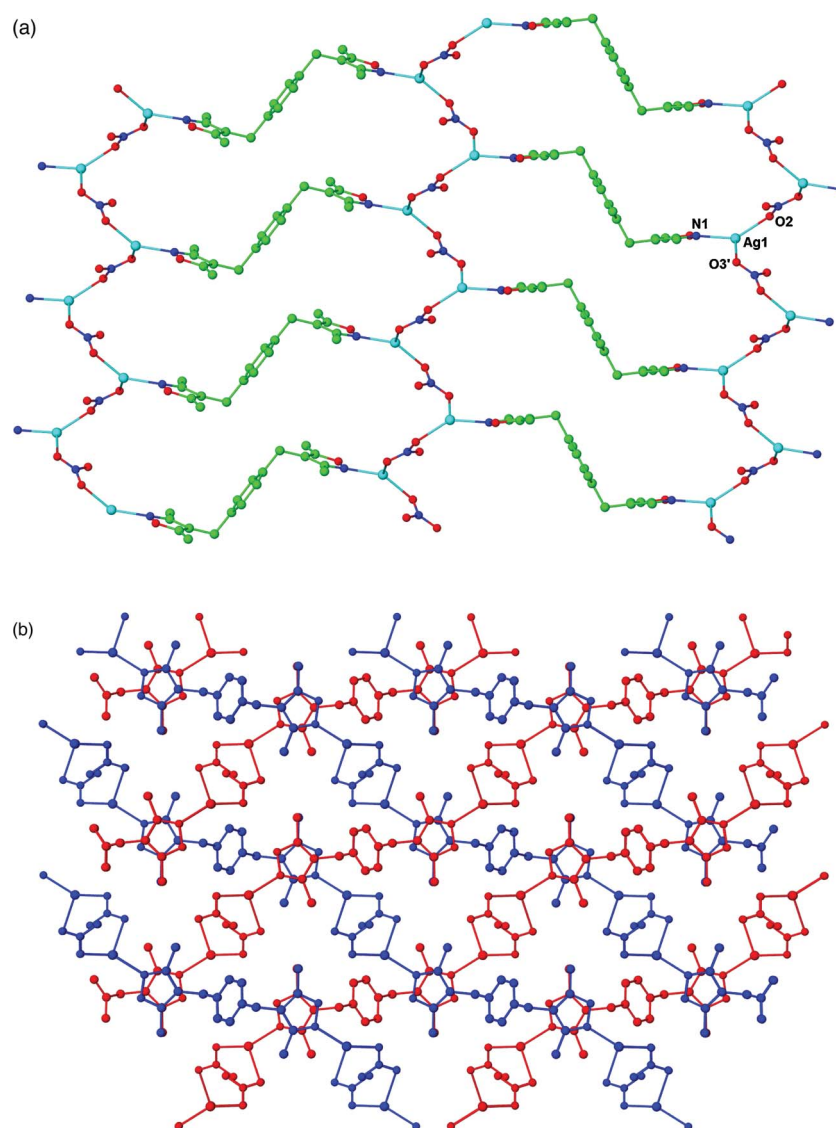


Fig. 2 The structure of $[\text{Ag}_2(\text{NO}_3)_2(\text{bisox})]$ **1** showing (a) the sheet structure, and (b) the 2D inclined interpenetration of the sheets. Hydrogen atoms have been removed for clarity. Selected bond lengths and angles: $\text{Ag}(1)\text{--}\text{N}(1)$ 2.195(3), $\text{Ag}(1)\text{--}\text{O}(2)$ 2.307(3), $\text{Ag}(1)\text{--}\text{O}(3')$ 2.468(3) Å, $\text{N}(1)\text{--}\text{Ag}(1)\text{--}\text{O}(2)$ 137.42(10), $\text{N}(1)\text{--}\text{Ag}(1)\text{--}\text{O}(3')$ 101.16(10), $\text{O}(2)\text{--}\text{Ag}(1)\text{--}\text{O}(3')$ 116.93(9) $^\circ$. Primed atoms generated by the symmetry operation $x + 1/2, -y + 1, -z + 1/2$.

Reaction of silver(I) trifluoroacetate and bisox

The reaction between bisox and silver(I) trifluoroacetate in methanol gave $[\text{Ag}(\text{O}_2\text{CCF}_3)(\text{bisox})]\cdot 0.5\text{MeOH}$ **2a**. The asymmetric unit of **2a** contains a silver(I) centre, a trifluoroacetate anion, coordinated by one of its oxygen atoms, two independent halves of bisox ligand and a fraction of an included methanol molecule. The remaining halves of the bisox ligands are generated by symmetry, and as with **1**, the ligands adopt *S*- conformations. A symmetry centre proximate to the silver centre leads to the formation of $\text{Ag}_2(\mu\text{-O}_2\text{CCF}_3)_2$ dimers, with a $\text{Ag}\cdots\text{Ag}$ distance of 3.0640(5) Å. Each silver centre is 4-coordinate, and bonded to two bisox ligands in addition to the oxygen atoms of two carboxylates. This means that each $\text{Ag}_2(\mu\text{-O}_2\text{CCF}_3)_2$ dimeric unit acts as a 4-connecting node, with a distorted square-planar geometry, as shown in Fig. 3a.

The bridging bisox ligands link the dimers into a (4,4)-connected two-dimensional grid as shown in Fig. 3b, containing 64-membered metallomacrocyclic rings. These rings are supported by $\text{C}\text{--}\text{H}\cdots\text{O}$ hydrogen bonds [$\text{C}(14)\cdots\text{O}(4)$ 3.355 Å, $\text{H}(14\text{A})\cdots\text{O}(4)$ 2.40 Å, $\text{C}(14)\text{--}\text{H}(14\text{A})\cdots\text{O}(4)$ 165 $^\circ$]. A combination of the partial occupancy methanol molecules and interdigitation by the trifluoroacetate groups of neighbouring sheets fill the rings and reduces the potential for porosity within the structure. The included methanol molecules also form hydrogen bonds with the fluorine atoms of the trifluoroacetate groups. $\text{Ag}_2(\text{O}_2\text{CCF}_3)_2\text{N}_4$ units such as those observed in **2a** have been observed previously in discrete structures,²¹ but this is the first example in an extended network.

Recrystallisation of **2a** from a acetonitrile–diethyl ether mixture gave crystals of $[\text{Ag}(\text{O}_2\text{CCF}_3)(\text{bisox})]\cdot 0.5\text{MeCN}$ **2b**, which has a similar gross structure to that of **2a**. Analysis of the unit cell

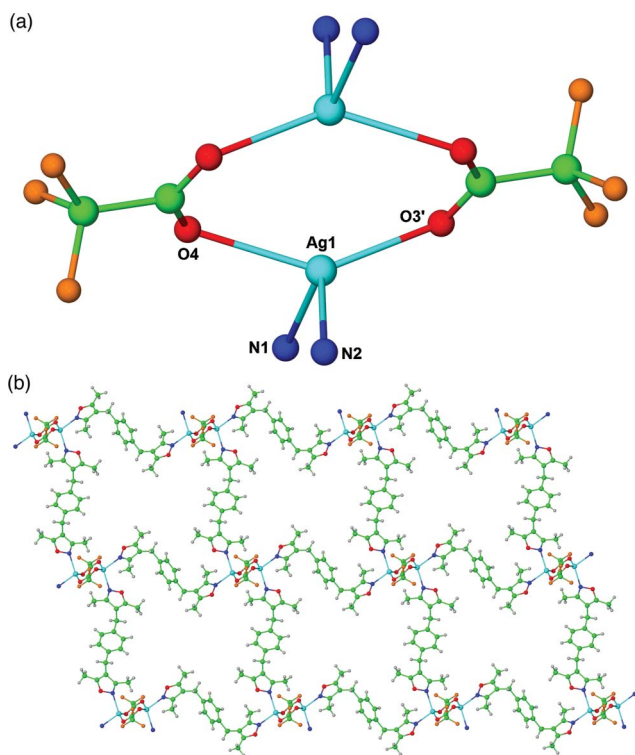


Fig. 3 The structure of $[\text{Ag}(\text{O}_2\text{CCF}_3)(\text{bisox})]\cdot 0.5\text{MeOH}$ **2**, showing (a) the dimeric $\text{Ag}_2(\text{O}_2\text{CCF}_3)_2$ unit and (b) the sheet structure. Included methanol molecules and minor disordered anion components have been removed for clarity. Selected bond lengths and angles: $\text{Ag}(1)\text{--N}(1)$ 2.335(3), $\text{Ag}(1)\text{--N}(2)$ 2.337(3), $\text{Ag}(1)\text{--O}(4)$ 2.377(3), $\text{Ag}(1)\text{--O}(3')$ 2.303(3) Å, $\text{N}(1)\text{--Ag}(1)\text{--N}(2)$ 108.25(10), $\text{O}(3')\text{--Ag}(1)\text{--N}(1)$ 99.88(10), $\text{O}(3')\text{--Ag}(1)\text{--N}(2)$ 116.19(12), $\text{N}(1)\text{--Ag}(1)\text{--O}(4)$ 91.07(9), $\text{N}(2)\text{--Ag}(1)\text{--O}(4)$ 95.35(11), $\text{O}(3')\text{--Ag}(1)\text{--O}(4)$ 140.68(11) $^\circ$. Primed atoms generated by the symmetry operation $-x + 1, -y + 2, -z + 1$.

parameters reveals one of the cell lengths of **2a** is approximately twice that of the corresponding parameter in **2b**.

Reaction between silver(I) perchlorate and bisox

The reaction between bisox and silver(I) perchlorate in methanol gave crystals of $[\text{Ag}_2(\text{bisox})_3](\text{ClO}_4)_2$ **3**, whereas recrystallisation of the crude product from acetonitrile–diethyl ether gave the diethyl ether solvate $[\text{Ag}_2(\text{bisox})_3](\text{ClO}_4)_2\cdot\text{Et}_2\text{O}$ **4**.

The asymmetric unit of **3** contains a third of a silver(I) centre, located on a three-fold rotation axis, half of a bisox ligand, proximate to an inversion centre, and a perchlorate anion fragment, in which the chlorine and one oxygen atom are located on the three-fold rotation axis. Each silver(I) centre is trigonal planar and coordinated to three bisox ligands. The bisox ligands adopt S-conformations, and link the silver centres into (6,3) sheets, as shown in Fig. 4a. The hexagonal ‘pores’ within these sheets have internal widths of 16.8 Å, and unsurprisingly interpenetration occurs to reduce the free space. The structure is triply parallel interpenetrated as shown in Fig. 4b. The layers contain Borromean links, which involve three interlocked rings. The triangular pores generated by this interpenetration are sandwiched between perchlorate anions, which are involved in $\text{C}\text{--H}\cdots\text{O}$ hydrogen bonds with both methyl and aromatic CH groups, as shown in Fig. 4c.

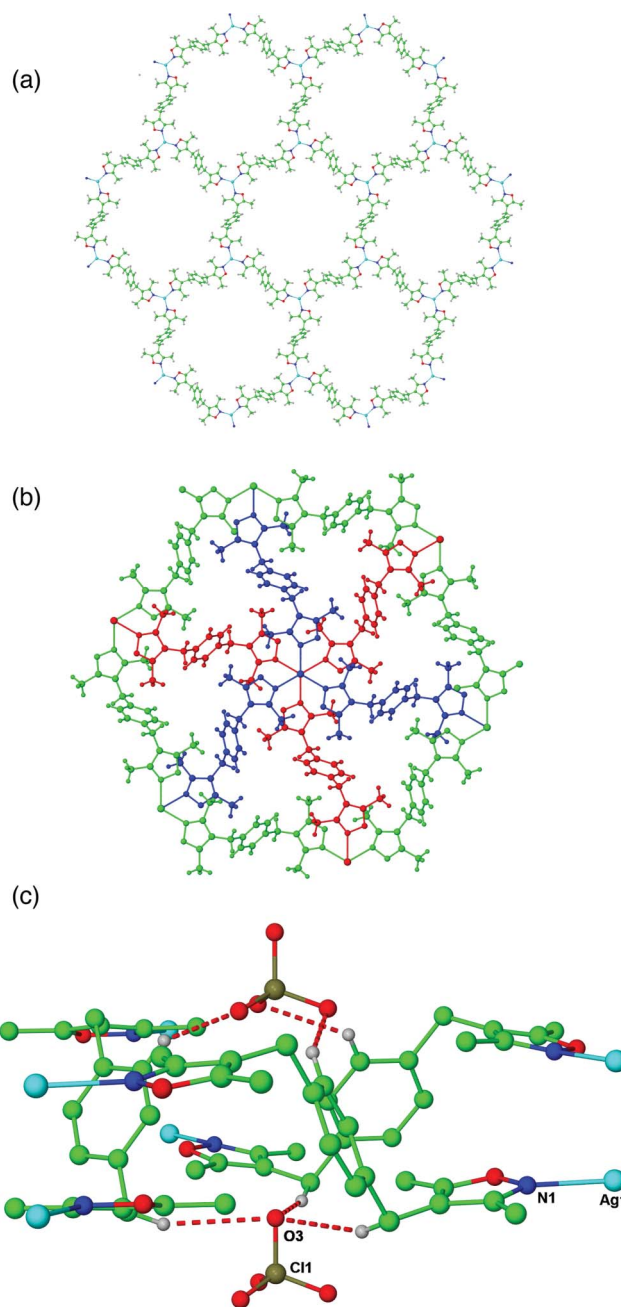


Fig. 4 The structure of $[\text{Ag}_2(\text{bisox})_3](\text{ClO}_4)_2$ **3** showing (a) one of the (6,3) $\text{Ag}_2(\text{bisox})_3$ layers present in the structure, (b) the triply interpenetrated network with the independent sheets shown in different colours, and (c) the position of the perchlorate anions with respect to the triangular pores, with $\text{C}\text{--H}\cdots\text{O}$ hydrogen bonds shown in red and white, and the hydrogen atom groups not involved in these interactions omitted for clarity. Selected bond lengths and angles: $\text{Ag}(1)\text{--N}(1)$ 2.225(2) Å, $\text{N}(1)\text{--Ag}(1)\text{--N}(1')$ 119.888(7) $^\circ$. Primed atoms generated by the symmetry operation $-y, x - y, z$.

The structure of **3** is similar to that observed previously for the 1,4-bis(2-methylimidazol-1-ylmethyl)benzene (bismim) networks $[\text{Ag}_2(\text{bismim})_3](\text{BF}_4)_2$ and $[\text{Ag}_2(\text{bismim})_3](\text{CF}_3\text{SO}_3)_2$.^{14,22} Subtle differences were seen in the two silver-bismim networks, with a change in orientation of the methylimidazolyl rings facilitating the presence of the larger triflate anion at the expense of $\text{Ag}\cdots\text{Ag}$ interactions. The bisox ligand has methyl groups on both sides

of the five-membered ring, and lies approximately parallel to the silver coordination plane. The $\text{Ag} \cdots \text{Ag}$ distance in **3** is 2.9990(7) Å, consistent with a $d^{10} \cdots d^{10}$ interaction.

The asymmetric unit of **4** contains two partial silver atoms, with one-third occupancy, two independent ligand halves proximate to inversion centres, two perchlorate fragments (central chlorines one-third occupancy) and a diethyl ether molecule with one-third occupancy. This generates the overall formula for **4** as $[\text{Ag}_2(\text{bisox})_3](\text{ClO}_4)_2 \cdot \text{Et}_2\text{O}$. Both independent silver centres have trigonal planar geometry, coordinated to three symmetry-related bisox ligands. However, the two independent bisox ligands have different conformations, with that coordinated to Ag(2) in the S- conformation, whereas that coordinated to Ag(1) is in the C- conformation. As a consequence, Ag(2) forms triply parallel interpenetrated (6,3) sheets similar to those in **3**, whereas Ag(1) forms discrete $\text{Ag}_2(\text{bisox})_3$ cages, as depicted in Fig. 5a. The diethyl ether molecules project through the faces of these cages.

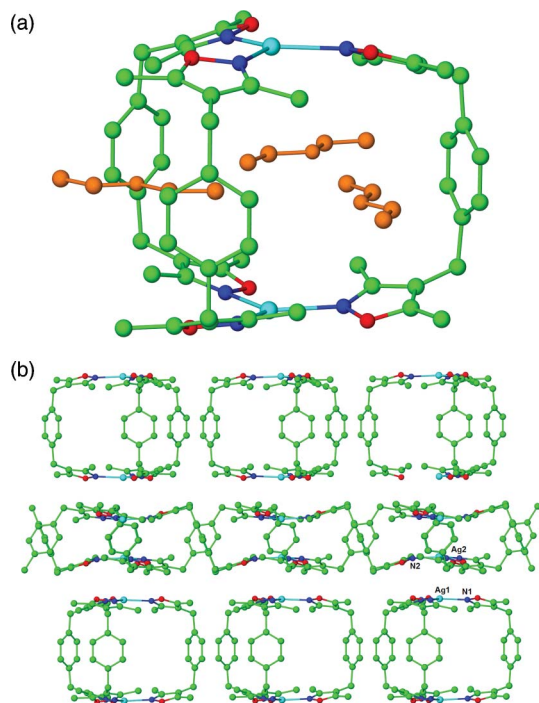


Fig. 5 The structure of $[\text{Ag}_2(\text{bisox})_3](\text{ClO}_4)_2 \cdot \text{Et}_2\text{O}$ **4**, showing (a) the $\text{Ag}_2(\text{bisox})_3$ cages, with the included diethyl ether molecules shown in orange, and (b) the alternation of triply interpenetrated sheets with rows of cages. Perchlorate anions and hydrogen atoms have been omitted for clarity. Selected bond lengths and angles: $\text{Ag}(1)\text{--N}(1)$ 2.234(4), $\text{Ag}(2)\text{--N}(2)$ 2.216(4) Å, $\text{N}(1)\text{--Ag}(1)\text{--N}(1')$ 119.841(14), $\text{N}(2)\text{--Ag}(2)\text{--N}(2')$ 119.745(17)°. Primed atoms generated by the symmetry operation $-y + 1, x - y - 1, z$.

In the gross structure, the $\text{Ag}_2(\text{bisox})_3$ cages lie directly above the silver centres of the interpenetrated sheets forming layers, as shown in Fig. 5b. As a consequence, there are two types of short $\text{Ag} \cdots \text{Ag}$ contact—those between the silver atoms within the sheets [$\text{Ag}(2) \cdots \text{Ag}(2')$ 3.0444(11) Å ($\text{Ag}(2')$ generated by symmetry operation $x + 2, -y, -z + 1$)] and those between a silver atom in a sheet and a silver atom in a cage [$\text{Ag}(1) \cdots \text{Ag}(2)$ 3.3253(8) Å]. The distance between the two silver atoms in a $\text{Ag}_2(\text{bisox})_3$ cage is 8.004(1) Å. The perchlorate anions occupy

positions to either side of the interpenetrated sheets, and are involved with $\text{C}\text{--H} \cdots \text{O}$ hydrogen bonds with CH donors on both the sheets and the cages.

Reaction of silver(i) tetrafluoroborate with bisox

The reactions of bisox with AgBF_4 proceed in a similar manner to the reactions with AgClO_4 . Thus the product from the reaction in methanol was $[\text{Ag}_2(\text{bisox})_3](\text{BF}_4)_2$ **5**, which exhibits a largely identical X-ray powder diffraction pattern to that of **3**. Recrystallisation of the crude methanol reaction product from acetonitrile–diethyl ether yielded the solvate $[\text{Ag}_2(\text{bisox})_3](\text{BF}_4)_2 \cdot 1.2\text{Et}_2\text{O}$ **6**, which is isostructural with **4**. In **6**, the portion of diethyl ether in the asymmetric unit refines to 0.40 occupancy, giving a slightly greater proportion of included solvent in the structure than in **4**, but otherwise there are no significant differences between the structures.

Ag_2L_3 cages have not been reported for the related bisim ligands, though Ag_2L_2 macrocycles have been observed in the structures of $[\text{Ag}_2(\text{bismim})_2](\text{BF}_4)_2 \cdot 2\text{MeCN}$ ¹⁶ and $[\text{Ag}_2(\text{Fbism})_2](\text{BF}_4)_2 \cdot \text{H}_2\text{O} \cdot \text{MeOH}$ (Fbism = 1,1'-(perfluoro-1,4-phenylene)bis(methylene)-bis(1*H*-imidazole)).²³ Interestingly, the acetonitrile molecules in $[\text{Ag}_2(\text{bismim})_2](\text{BF}_4)_2 \cdot 2\text{MeCN}$ occupy the centre of the macrocycles, and can be removed by heating to 80 °C. The resulting desolvated material retains the crystal structure, and has been shown to adsorb N_2 , H_2 , CO_2 and CH_4 at 30 °C. $[\text{Ag}_2(\text{Fbism})_2](\text{PF}_6)_2 \cdot 2\text{MeCN}$ has recently been shown to lose solvent in a single-crystal-to-single-crystal transformation.²⁴

The reaction between silver(i) tetrafluoroborate and bisox was carried out in acetonitrile in the absence of diethyl ether to see whether analogous $\text{Ag}_2(\text{bisox})_2$ cages could be formed. However, the powder X-ray diffraction pattern of the product revealed it to be $[\text{Ag}_2(\text{bisox})_3](\text{BF}_4)_2$ **5**, which suggests that diethyl ether is important in templating formation of the $\text{Ag}_2(\text{bisox})_3$ cages.

Reaction of silver(i) hexafluorophosphate with bisox

The reaction of bisox with silver(i) hexafluorophosphate in methanol gave a mixture of products from which crystals of $[\text{Ag}(\text{bisox})_2]\text{PF}_6 \cdot 0.5\text{bisox}$ **7** were isolated. The asymmetric unit of **7** contains one silver centre, two and a half bisox molecules and one hexafluorophosphate anion. The two complete bisox molecules adopt C-shaped conformations and are coordinated, bridging between silver centres. Each silver centre coordinates to four ligands, and adopts a distorted tetrahedral geometry, with bond angles ranging from 100.14(7) to 117.09(7)°. The bisox ligands connect the silver centres into one-dimensional chains of macrocycles, as shown in Fig. 6. The remaining bisox molecules, generated from the half molecule in the asymmetric unit, are uncoordinated, and lie within half of the macrocyclic rings, so that alternate rings are filled and empty. The uncoordinated bisox molecules are in the S- conformation. The hexafluorophosphate anions lie between the chains.

7 can be regarded as a polyseudorotaxane, and it has some features in common with the two-dimensional polyrotaxane network formed by $[\text{Ag}_2(\text{bism})_3](\text{NO}_3)_2$ (bism = 1,4-bis(imidazol-1-ylmethyl)benzene).¹³ In this compound, similar macrocyclic rings to those seen in **7** also encompass additional ligands, although in the bisim case, in contrast to **7**, the additional ligands are coordinated.

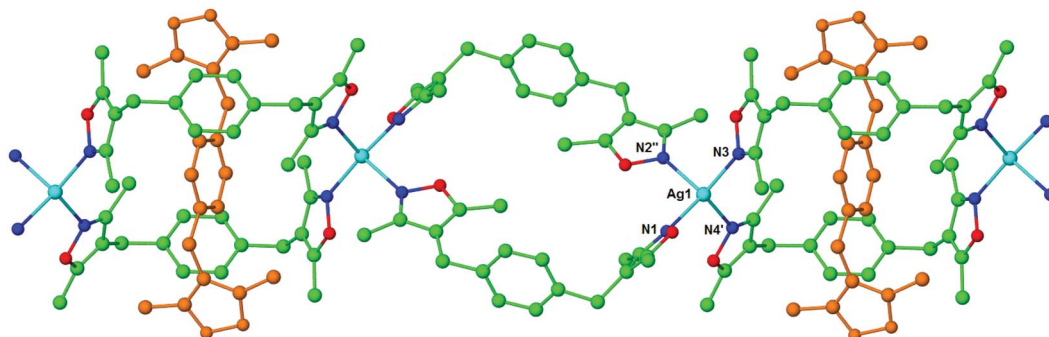


Fig. 6 The structure of $[\text{Ag}(\text{bisox})_2]\text{PF}_6 \cdot 0.5\text{bisox}$ **7** showing the one-dimensional chains and the included bisox molecules. Hydrogen atoms are omitted for clarity, and included bisox molecules are shown in orange. Selected bond lengths and angles: $\text{Ag}(1)\text{--N}(1)$ 2.2813(19), $\text{Ag}(1)\text{--N}(3)$ 2.2532(19), $\text{Ag}(1)\text{--N}(4)'$ 2.2983(19), $\text{Ag}(1)\text{--N}(2)''$ 2.348(2) Å, $\text{N}(3)\text{--Ag}(1)\text{--N}(1)$ 114.72(7), $\text{N}(3)\text{--Ag}(1)\text{--N}(4)'$ 117.09(7), $\text{N}(1)\text{--Ag}(1)\text{--N}(4)'$ 111.42(7) $\text{N}(3)\text{--Ag}(1)\text{--N}(2)''$ 105.55(7), $\text{N}(1)\text{--Ag}(1)\text{--N}(2)''$ 105.97(7), $\text{N}(4)'\text{--Ag}(1)\text{--N}(2)''$ 100.14(7)°. Primed atoms generated by the symmetry operation $-x + 1, -y, -z$. Double primed atoms generated by the symmetry operation $-x + 3, -y + 1, -z + 1$.

Reaction of silver(I) hexafluoroantimonate with bisox

The reaction of bisox with silver(I) hexafluoroantimonate in methanol gave a mixture of products from which crystals of $[\text{Ag}(\text{bisox})_2]\text{SbF}_6 \cdot 0.5\text{bisox}$ **8** were isolated. These were shown by an X-ray single crystal analysis to be isostructural with **7**, so will not be discussed further. The crude reaction mixture was recrystallised from acetonitrile–diethyl ether to give $[\text{Ag}(\text{bisox})_2]\text{SbF}_6$ **9** as the sole product. The asymmetric unit of **9** consists of one silver centre located on a crystallographic two-fold axis, two independent ligand halves, the remainder of each generated *via* an inversion centre in the middle of the six-membered ring, and half of a hexafluoroantimonate anion fragment with the central atom located at an inversion centre. Each silver centre coordinates to four ligands, and adopts a distorted tetrahedral geometry, as shown in Fig. 7a, with bond angles ranging from 94.46(8) to 126.85(6)°. The bisox ligands adopt S- conformations, and link the silver centres into a three-dimensional flattened diamondoid network, as shown in Fig. 7b. This is triply-interpenetrated, as shown in Fig. 7c. The SbF_6^- anions are accommodated in cavities, and interact with the network through $\text{C--H} \cdots \text{F}$ hydrogen bonds involving the methyl and methylene groups.

Reaction of silver(I) triflate with bisox

The reaction of bisox with silver(I) triflate in methanol gave $[\text{Ag}(\text{bisox})_2]\text{CF}_3\text{SO}_3$ **10**, which is isostructural to **9**. The anion lies on an inversion centre, which ensures disorder between the two halves. It is involved in $\text{C--H} \cdots \text{O/F}$ hydrogen bonds.

Discussion

Analysis of the crystal structures of **1–4** and **6–10** reveals a number of interesting features. The nitrate and trifluoroacetate anions are well established as being able to coordinate to silver(I) centres,⁹ and the products from the reactions between bisox and AgNO_3 or AgO_2CCF_3 both contain Ag-anion bonds. Indeed, these bonds play an important role in determining the structures of these compounds, and the ability of a carboxylate to bridge metal centres into dimers is evident in the structures of **2a** and **2b**.

The tetrahedral anions ClO_4^- and BF_4^- give the isostructural triply-interpenetrated sheet structures **3** and **5**. Similar sheets are

formed using the related bis(pyrazolyl) ligand *bisim*,^{14,22} and in all cases the interweaving is facilitated by the relative positions of the nitrogen donors in the S- conformation of both bisox and *bisim*. The size and shape of the ClO_4^- and BF_4^- ions are important in forming this structure, with the anions located proximate to the triangular pores and involved in $\text{CH} \cdots \text{X}$ interactions.

Recrystallisation of **3** and **5** from acetonitrile–diethyl ether gives compounds **4** and **6**, the structures of which contain discrete Ag_2L_3 cages in addition to sheets. These cages are not observed in the absence of diethyl ether, and the proximity of the Et_2O molecules to the cages in the structures of **4** and **6** suggest the diethyl ether molecules play a templating role. This is further evidenced by the fact that carrying out the reaction between silver(I) tetrafluoroborate and bisox in acetonitrile generates **5**, in which the Ag_2L_3 cages are absent. $\text{Ag} \cdots \text{Ag}$ interactions may be important in stabilising the structures of **3–6**. $\text{Ag} \cdots \text{Ag}$ distances of 2.9990(7), 3.0444(11) and 3.0597(12) Å were observed between the interwoven sheets in **3**, **4** and **6** respectively, whereas $\text{Ag} \cdots \text{Ag}$ distances of 3.3253(8) and 3.3236(9) Å were observed between the sheets and cages in **4** and **6**.

The triply interpenetrated sheets observed in **3–6** are not observed when using silver salts containing larger anions. The lack of tetrahedral symmetry may also be a factor, as formation of the $\text{C--H} \cdots \text{X}$ interactions between the ligands and the anions would orientate an octahedral anion or triflate in a sterically unfavourable position, disfavoured formation of this structural type with respect to one-dimensional chains in the case of **7** and **8**, or three dimensional diamondoid structures in the cases of **9** and **10**.

In order to see whether silver-bisox fragments would preferentially crystallise with a particular anion, reactions between bisox and a mixture of silver(I) salts were studied. In all cases, the powder X-ray diffraction patterns suggested these reactions yielded mixtures of products, suggesting selective crystallisation does not occur with this series of compounds.

Solid state interconversions

Rearrangement of coordination networks *via* dissolution-precipitation pathways is well established,²⁵ though solid state transformations are less common, and typically involve a change in

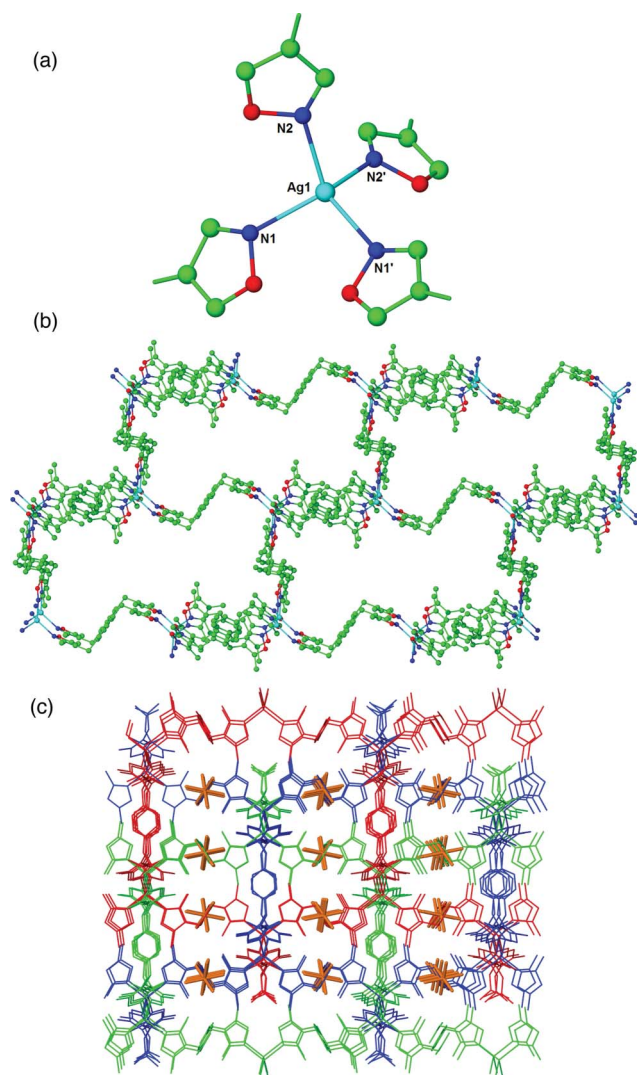


Fig. 7 The structure of $[\text{Ag}(\text{bisox})_3]\text{SbF}_6$ **9** showing (a) the geometry about the silver(i) centre, (b) one of the flattened diamondoid networks, and (c) the three triply-interpenetrated networks shown in different colours, with the hexafluoroantimonate ions in orange and hydrogen atoms omitted for clarity. Selected bond lengths and angles: $\text{Ag}(1)\text{--N}(1)$ 2.3089(15), $\text{Ag}(1)\text{--N}(1)'$ 2.3089(15), $\text{Ag}(1)\text{--N}(2)$ 2.3075(15), $\text{Ag}(1)\text{--N}(2)'$ 2.3075(15) Å, $\text{N}(2)\text{--Ag}(1)\text{--N}(1)$ 103.71(5), $\text{N}(1)\text{--Ag}(1)\text{--N}(1)'$ 103.92(7), $\text{N}(2)\text{--Ag}(1)\text{--N}(2)'$ 94.46(8), $\text{N}(2)'\text{--Ag}(1)\text{--N}(1)$ 126.85(6), $\text{N}(2)\text{--Ag}(1)\text{--N}(1)'$ 126.85(6), $\text{N}(2)'\text{--Ag}(1)\text{--N}(1)'$ 103.71(5)°. Primed atoms generated by the symmetry operation $-x + 3, y, -z + 1/2$.

the metal coordination environments.²⁶ Interconversions between 1D, 2D and 3D silver-polynitrile coordination polymers have been shown to be promoted by anion exchange,²⁷ whereas conversion between 1D ladders and 2D bilayers in the $[\text{Zn}_2(4,4'\text{-bipy})_3(\text{NO}_3)_4]$ system has been facilitated by inclusion of guest molecules.²⁸ Dehydration of networks based on tris(carboxyethyl)isocyanurate²⁹ and 5-sulfoisophthalate³⁰ have both been demonstrated to initiate reversible transformations involving additional coordination of donor atoms from the ligands.

Compounds $[\text{Ag}_2(\text{bisox})_3](\text{ClO}_4)_2$ **3** and $[\text{Ag}_2(\text{bisox})_3](\text{ClO}_4)_2 \cdot \text{Et}_2\text{O}$ **4** have similar compositions and possess structural features in common. Hence, it was of interest to see whether the diethyl ether

solvate molecules in **4** could be removed to leave empty cages, or whether loss of solvent would facilitate a structural rearrangement.

The initial X-ray powder diffraction for **4** suggested the compound was phase pure, with no other crystalline compounds observed. The TGA is also consistent with the presence of the Et_2O molecules. A mass loss of 2.7% was observed between 100 and 120 °C which corresponds to the removal of half of the diethyl ether. The remainder of the solvent is lost more gradually, with the network decomposition beginning at around 280 °C.

A powdered sample of **4** was placed under vacuum for 4 h, and then heated at 50 °C under vacuum for 4 h. During this time, a powder X-ray diffraction pattern was recorded every hour. These were all identical to that observed initially for **4**, signifying no structural rearrangement had occurred. TGA on the heated samples confirmed that diethyl ether was still present, confirming that no change had occurred. The sample was then heated at 75 °C under vacuum for 4 h, with a powder X-ray diffraction pattern again recorded every hour. These patterns revealed that a gradual conversion of **4** into **3** was occurring (Fig. 8) which was completed after 4 h. The conversion appears to be clean, with no other products observed in the powder diffraction traces. The TGA confirmed the complete loss of the solvent, and furthermore showed no mass loss until the onset of decomposition at 280 °C.

The conversion of **4** into **3** involves a significant rearrangement of the network, so is remarkable given the material remains crystalline throughout, although single crystals do not survive this transformation. The bisox ligand is required to rearrange from the C-conformation in **4** to the S-conformation in **5**, which requires a rotation of 180° of one of the isoxazolyl rings about a methylene carbon atom. This, in turn, involves the ring nitrogen atom moving through an arc of approximately 10.7 Å. This change also requires breaking and re-forming of half of the Ag–N bonds (Fig. 9). The conversion of the cages into the 2D sheets also necessitates a substantial movement of the silver atoms, which is consistent with a 17% shrinkage in the *c* direction of the cell.

A similar investigation was carried out with the isostructural tetrafluoroborate analogue $[\text{Ag}_2(\text{bisox})_3](\text{BF}_4)_2 \cdot 1.2\text{Et}_2\text{O}$ **6**. In this case, conversion of **6** into $[\text{Ag}_2(\text{bisox})_3](\text{BF}_4)_2$ **5** occurs more readily than with the perchlorate compounds **4** and **3**, and does not require any heating. Indeed, a crystalline sample of **6** was shown by powder X-ray diffraction to convert completely into **5** on standing in the atmosphere for 1 week at room temperature. This conversion was speeded up by placing the sample under vacuum—after 1 h a sample of **6** had been almost completely converted to **5**, and after 3 h under vacuum the transformation was complete.

The more facile loss of diethyl ether from **6** when compared with **4** may be related to differences in the intermolecular interactions. Although the diethyl ether molecules reside in very similar positions in the cages of **4** and **6**, the intermolecular contacts with the anions are slightly shorter in the perchlorate case. Thus for **4**, there are two C–H...O interactions $[\text{C}(102)\cdots\text{O}(5)$ 3.935, $\text{H}(10\text{E})\cdots\text{O}(5)$ 3.04 Å, $\text{C}(102)\text{--H}(10\text{E})\cdots\text{O}(5)$ 153°] whereas for **6** there are two longer C–H...F interactions $[\text{C}(23)\cdots\text{F}(2)$ 4.032, $\text{H}(23\text{B})\cdots\text{F}(2)$ 3.16 Å, $\text{C}(23)\text{--H}(23\text{B})\cdots\text{F}(2)$ 149°].

Conclusions

By using the semi-rigid ligand bisox, silver coordination polymers with a wide range of structures were formed including examples

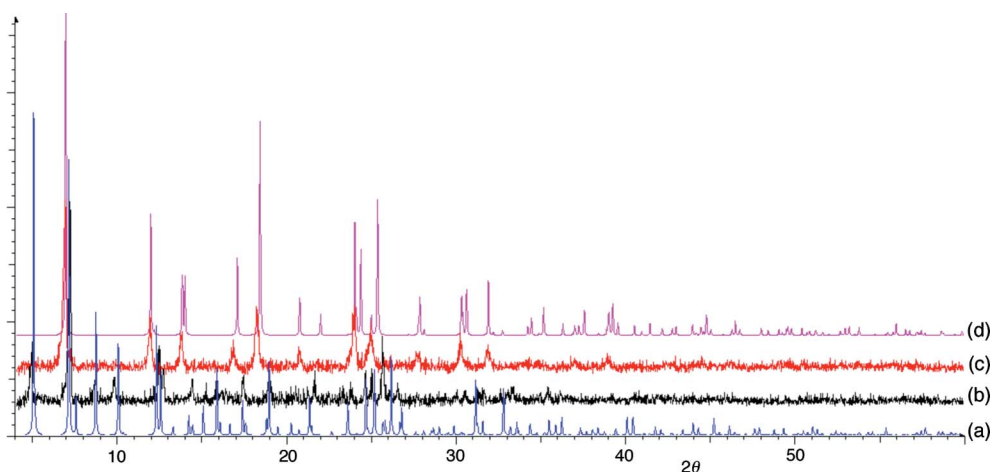


Fig. 8 Powder X-ray diffraction patterns for the conversion of **4** into **3**: (a) Simulated pattern for **4**, (b) **4**, (c) **4** heated at 75 °C under vacuum for 1 h, (d) simulated pattern for **3**.

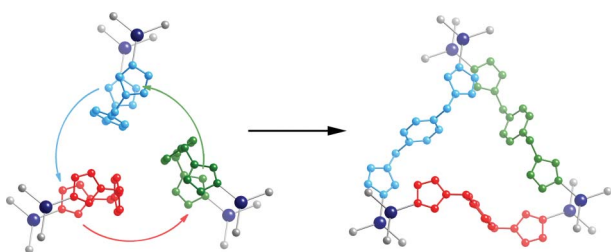


Fig. 9 The transformations required to convert the $\text{Ag}_2(\text{bisox})_3$ cages in **4** and **6** into the triply-interpenetrated sheets in **3** and **5**.

with zero-, one-, two- and three-dimensional networks. The occurrence of two distinct ligand conformations is a factor in the broad structural chemistry observed, though the anion was also shown to play a major role in determining the structure adopted. The most unusual feature in this series of compounds is the ability of diethyl ether to template the formation of $\text{Ag}_2(\text{bisox})_3$ cages in the solid state, leading to materials containing both interwoven sheets and discrete cages.

Removal of the included diethyl ether molecules was observed for both $[\text{Ag}_2(\text{bisox})_3](\text{ClO}_4)_2 \cdot \text{Et}_2\text{O}$ **4** and $[\text{Ag}_2(\text{bisox})_3](\text{BF}_4)_2 \cdot 1.2\text{Et}_2\text{O}$ **6**, with the former requiring more forcing conditions. In both cases, the powder X-ray diffraction data shows that solvent loss occurs with a solid state transformation to give $[\text{Ag}_2(\text{bisox})_3](\text{ClO}_4)_2$ **3** and $[\text{Ag}_2(\text{bisox})_3](\text{BF}_4)_2$ **5** respectively. These conversions involve rearrangement of cages into sheets, and are accompanied by a change in conformation of half of the bisox ligands from the C- to the S- conformation.

Experimental

General

3,3'-(1,4-Phenylenebis(methylene))bis(4-hydroxypent-3-en-2-one) was prepared following the previously reported method.¹⁹ All other compounds were obtained commercially and used without further purification.

Powder diffraction measurements were recorded using a Bruker D8 powder diffractometer, fitted with Goebel mirrors, and using Cu-K α radiation of wavelength 1.5414 Å. Samples were placed in 0.3 mm to 0.7 mm diameter Lindemann capillaries, and measured with a 2θ range of 4–60°. The step size was 0.02° with time per step of 1.00 s.

Elemental analyses were conducted by Alan Carver (University of Bath) and Gillian Maxwell (University College London). NMR spectra were recorded at 298 K on a Bruker Avance 300 MHz NMR spectrometer, and referenced to residual *protio* solvent signals for ^1H NMR spectra (CDCl_3 , δ 7.24) and to solvent resonances for $^{13}\text{C}\{^1\text{H}\}$ NMR (CDCl_3 , δ 77.2). Mass spectra were recorded on a Bruker MicrOTOF electrospray time-of-flight (ESI-TOF) mass spectrometer (Bruker Daltonik GmbH) coupled to an Agilent 1200 LC system (Agilent Technologies). Thermogravimetric analyses were recorded on a Perkin Elmer TGA 4000 analyser heating at 5 °C min^{-1} under an atmosphere of nitrogen.

Safety note: Although no issues were observed during the course of this study, care must be taken with using perchlorates as they are potentially explosive.

Synthesis of 1,4-bis((3,5-dimethylisoxazol-4-yl)methyl)benzene (bisox)

Hydroxylamine hydrochloride (2.11 g, 30 mmol), dissolved in 1 N NaOH solution (20 cm^3 , 20 mmol), was added to 3,3'-(1,4-phenylenebis(methylene))bis(4-hydroxypent-3-en-2-one) (4.08 g, 13.5 mmol) suspended in EtOH (50 cm^3) at room temperature. The mixture was heated at reflux for 3 h and the solvents removed under reduced pressure. The residue was suspended in H_2O (100 cm^3) and the pH adjusted to 7. The solid material was collected by filtration, washed with H_2O ($3 \times 20 \text{ cm}^3$) and crystallised from hot EtOH– H_2O . Yield 3.59 g (89%). Found: C, 72.9; H, 6.78; N, 9.31. $\text{C}_{18}\text{H}_{20}\text{N}_2\text{O}_2$ requires C, 72.9; H, 6.81; N, 9.46. δ_{H} (300 MHz; CDCl_3) 2.06 (6 H, s), 2.28 (6 H, s), 3.63 (4 H, s), 7.06 (4 H, s). δ_{C} (75.5 MHz, CDCl_3) 10.27, 10.96, 27.67, 112.26, 128.25, 136.95, 159.86, 165.32. m/z (ESI) 297.1586 ($[\text{M} + \text{H}]^+$). $[\text{C}_{18}\text{H}_{20}\text{N}_2\text{O}_2 + \text{H}]^+$ requires 297.1603.

Synthesis of $[\text{Ag}_2(\text{NO}_3)_2(\text{bisox})] \mathbf{1}$

bisox (0.029 g, 0.10 mmol) was dissolved in methanol (2 cm³) with gentle heating and stirring. To this solution, AgNO₃ (0.017 g, 0.10 mmol) dissolved in methanol (1 cm³) was added, rinsing through with a further 0.5 cm³ methanol. The solution was stood at room temperature overnight. A small amount of a brown precipitate had formed, which was removed by filtration through a cotton wool plug. The solution was left at room temperature for 3 days, with the vial lid slightly open to allow approximately half of the solvent to evaporate slowly. The crystalline product was then separated by filtration and washed with small amounts of methanol. Yield 0.033 g. The crude product was recrystallised by dissolving in the minimum amount of MeCN and allowing Et₂O to diffuse slowly into the solution. Crystals of suitable size for single crystal X-ray analysis began to form after several days. The X-ray powder diffraction pattern showed **1** to be the major product, with an unidentified by-product also present.

Synthesis of $[\text{Ag}(\text{O}_2\text{CCF}_3)(\text{bisox})] \cdot 0.5\text{MeOH} \mathbf{2a}$ and $[\text{Ag}(\text{O}_2\text{CCF}_3)(\text{bisox})] \cdot 0.5\text{MeCN} \mathbf{2b}$

bisox (0.029 g, 0.10 mmol) was dissolved in methanol (2 cm³) with gentle heating and stirring. To this solution, AgCF₃CO₂ (0.022 g, 0.10 mmol) dissolved in methanol (1 cm³) was added, rinsing through with a further 0.5 cm³ methanol. The solution was allowed to stand at room temperature overnight. A small amount of a brown precipitate had formed, which was removed by filtration through a cotton wool plug. The solution was left at room temperature for approximately 3 days, with the vial lid slightly open to allow slow evaporation of the solvent. Crystals of **2a** were formed which were of suitable size for single crystal X-ray analysis. Yield 0.024 g (45%). Found: C, 46.20; H, 4.15, N, 5.21. C_{20.5}H₂₂AgF₃N₂O_{4.5} requires C, 46.17; H, 4.16, N, 5.25%. Recrystallisation of the crude product from MeCN–Et₂O yielded crystals of **2b** which were suitable for single crystal X-ray analysis.

Synthesis of $[\text{Ag}_2(\text{bisox})_3](\text{ClO}_4)_2 \mathbf{3}$, and $[\text{Ag}_2(\text{bisox})_3](\text{ClO}_4)_2 \cdot \text{Et}_2\text{O} \mathbf{4}$

bisox (0.144 g, 0.49 mmol) was dissolved in methanol (10 cm³) with gentle heating and stirring. To this solution, AgClO₄ (0.050 g, 0.24 mmol) dissolved in methanol (3 cm³) was added. The product was allowed to crystallise overnight. This solid product was filtered and washed with methanol. Yield 0.146 g (93%). Found: C, 49.54; H, 4.53; N, 5.91. C₅₄H₆₀Ag₂Cl₂N₆O₁₄ requires C, 49.75; H, 4.64; N, 6.45%. Compound **3** was recrystallised by dissolving it in the minimum volume of MeCN and allowing Et₂O to slowly diffuse into the solution. Crystals of suitable size were produced for single crystal X-ray diffraction. Found: C, 50.60; H, 4.74; N, 6.09. C₅₈H₇₀Ag₂Cl₂N₆O₁₅ requires C, 50.56; H, 5.12; N, 6.10%.

Synthesis of $[\text{Ag}_2(\text{bisox})_3](\text{BF}_4)_2 \mathbf{5}$, and $[\text{Ag}_2(\text{bisox})_3](\text{BF}_4)_2 \cdot 1.2\text{Et}_2\text{O} \mathbf{6}$

bisox (0.061 g, 0.2 mmol) was dissolved in methanol (6 cm³) with gentle heating and stirring. To this solution, AgBF₄ (0.021 g, 0.1 mmol) dissolved in methanol (1 cm³) was added. The product was allowed to crystallise overnight. The crystalline product was separated by filtration and washed with small amounts of

methanol. Yield 0.031 g (48%). Found: C, 50.02; H, 4.57; N, 6.57. C₅₄H₆₀Ag₂B₂F₈N₆O₆ (**5**) requires C, 50.73; H, 4.73; N, 6.57%. Compound **5** was recrystallised by dissolving it in the minimum volume of MeCN and allowing Et₂O to slowly diffuse into the solution. Crystals of the diethyl ether solvate **6** of suitable size were produced for single crystal X-ray diffraction.

Synthesis of $[\text{Ag}(\text{bisox})_2]\text{PF}_6 \cdot 0.5\text{bisox} \mathbf{7}$

bisox (0.073 g, 0.25 mmol) was dissolved in methanol (4 cm³) with gentle heating and stirring. To this solution, AgPF₆ (0.031 g, 0.12 mmol) dissolved in methanol (2 cm³) was added. The product was allowed to crystallise overnight. The solid product was filtered, and washed with the minimum quantity of methanol. Crystals of suitable size were produced from the methanol filtrate for single crystal X-ray diffraction. The X-ray powder diffraction pattern revealed that **7** was not the only product of the reaction.

Synthesis of $[\text{Ag}(\text{bisox})_2]\text{SbF}_6 \cdot 0.5\text{bisox} \mathbf{8}$, and $[\text{Ag}(\text{bisox})_2]\text{SbF}_6 \mathbf{9}$

bisox (0.060 g, 0.2 mmol) was dissolved in methanol (6 cm³) with gentle heating and stirring. To this solution, AgSbF₆ (0.036 g, 0.1 mmol) dissolved in methanol (1 cm³) was added. The product was allowed to crystallise overnight at room temperature. The crystalline product was then filtered and washed with small amounts of methanol. Crystals of $[\text{Ag}(\text{bisox})_2]\text{SbF}_6 \cdot 0.5\text{bisox} \mathbf{8}$ were isolated from the filtrate, though X-ray powder diffraction revealed the presence of another compound too. The crude product was recrystallised by dissolving it in the minimum amount of MeCN and allowing Et₂O to slowly diffuse into the solution. Powder X-ray diffraction confirmed that following recrystallisation, $[\text{Ag}(\text{bisox})_2]\text{SbF}_6 \mathbf{9}$ was the sole product. Found: C, 46.10; H, 4.31; N, 5.64. C₃₆H₄₀AgF₆N₄O₄Sb requires C, 46.18; H, 4.31; N, 5.98%.

Synthesis of $[\text{Ag}(\text{bisox})_2]\text{CF}_3\text{SO}_3 \mathbf{10}$

bisox (0.030 g, 0.10 mmol) was dissolved in methanol (2 cm³) with gentle heating and stirring. To this solution, AgCF₃SO₃ (0.023 g, 0.10 mmol) dissolved in methanol (1 cm³) was added, rinsing through with a further 0.5 cm³ methanol. The solution was allowed to stand at room temperature overnight. A small amount of a brown precipitate had formed, which was removed by filtration through a cotton wool plug. The solution was left at room temperature for approximately 3 days, with the vial lid slightly open to allow half of the solvent to evaporate slowly. Crystals formed which were suitable for single crystal X-ray analysis. Yield 0.026 g (34%). Found: C, 52.25; H, 4.73; N, 6.30. C₃₇H₄₀AgF₃N₄O₇S requires C, 52.30; H, 4.75; N, 6.59%.

Crystallography

X-ray data for compounds **1–4** and **6–10** were collected on a Nonius Kappa CCD diffractometer using Mo-K α radiation. Details of the data collections, solutions and refinements are given in Table 1. Unless noted below, all non-hydrogen atoms were refined anisotropically in the final least squares run, and hydrogen atoms were included at calculated positions. The structures were solved using SHELXS-97 and refined using full-matrix least squares in

Table 1 Crystal data and structure refinement for compounds 1–4 and 6–10

Compound	1	2a	2b	3	4	6	7	8	9	10
Formula	C ₁₈ H ₂₀ Ag ₂ N ₄ O ₈	C _{20.5} H _{22.5} AgF ₃ N _{4.5} O _{4.5}	C ₄₂ H ₄₃ Ag ₂ F ₆ N ₂ O ₈	C ₅₄ H ₆₀ Ag ₂ Cl ₂ N ₆ O ₁₄	C ₃₈ H ₇₀ Ag ₂ Cl ₂ N ₆ O ₁₅	C _{117.6} H ₁₄₄ Ag ₄ B ₂ F ₁₆ N ₁₂ O ₁₄₄	C ₄₅ H ₅₀ AgF ₆ N ₅ O ₃ P	C ₄₅ H ₅₀ AgF ₆ N ₅ O ₃ Sb	C ₃₆ H ₄₀ AgF ₆ N ₄ O ₃ Sb	C ₃₇ H ₄₀ AgF ₃ N ₄ O ₃ S
<i>M</i>	636.12	533.27	1075.55	1303.72	1377.84	2734.77	936.34	1084.52	936.34	849.66
<i>T/K</i>	150(2)	150(2)	150(2)	150(2)	150(2)	150(2)	150(2)	150(2)	150(2)	150(2)
Wavelength/Å	0.71073	0.71073	0.71073	0.71073	0.71073	0.71073	0.71073	0.71073	0.71073	0.71073
Crystal system	Orthorhombic	Triclinic	Triclinic	hexagonal	hexagonal	hexagonal	Triclinic	Triclinic	Monoclinic	Monoclinic
Space group	<i>Pcab</i>	<i>P1</i>	<i>P1</i>	<i>P</i> -3	<i>P6</i> / ₃ / <i>m</i>	<i>P6</i> / ₃ / <i>m</i>	<i>P1</i>	<i>P1</i>	<i>C2/c</i>	<i>C2/c</i>
<i>a</i> /Å	7.3890(1)	10.3470(2)	10.7180(2)	14.8380(3)	14.4400(2)	14.3960(2)	13.5620(1)	13.5300(3)	21.7220(3)	21.6760(3)
<i>b</i> /Å	15.9620(3)	11.2600(2)	11.2600(2)	14.8380(3)	14.4400(2)	14.3960(2)	14.2000(1)	14.3010(4)	11.4650(2)	11.3410(1)
<i>c</i> /Å	17.7590(4)	11.2920(2)	20.7660(5)	7.3050(1)	35.3990(6)	35.3830(7)	14.2460(2)	14.3670(3)	15.4820(2)	15.7510(2)
α (°)	90	64.703(1)	75.779(1)	90	90	90	103.616(1)	103.860(1)	90	90
β (°)	90	70.872(1)	81.104(1)	90	90	90	113.747(1)	113.574(1)	90	93.566(1)
γ (°)	90	82.471(1)	64.377(1)	120	120	120	103.917(1)	103.746(1)	90	90
<i>U</i> /Å ³	2094.55(7)	1082.09(3)	2187.07(8)	1392.84(4)	6392.28(17)	6350.51(18)	2260.62(4)	2293.51(9)	3852.31(10)	3864.53(8)
<i>Z</i>	4	2	2	1	4	2	2	2	4	4
μ /mm ⁻¹	1.925	0.989	0.978	0.869	0.763	0.694	0.556	1.090	1.281	0.642
Reflections collected	39756	22067	28707	20782	67463	43636	38548	38829	41679	36623
Independent reflections	2380 [R(int) = 0.0814]	6297 [R(int) = 0.0371]	7585 [R(int) = 0.0574]	2127 [R(int) = 0.0712]	3828 [R(int) = 0.1774]	4919 [R(int) = 0.0926]	10256 [R(int) = 0.0734]	10477 [R(int) = 0.0554]	5618 [R(int) = 0.0600]	4424 [R(int) = 0.0648]
Reflections observed (> 2 σ)	1687	5570	5709	1611	2001	2692	7231	7989	4492	3733
Goodness-of-fit on <i>F</i> ²	1.042	1.060	1.029	1.052	0.937	1.065	1.014	1.036	1.033	1.204
<i>R</i> ₁ , <i>wR</i> ₂ [<i>I</i> > 2 σ (<i>I</i>)]	0.0359, 0.0868	0.0485, 0.1344	0.0416, 0.0899	0.0362, 0.0808	0.0455, 0.1075	0.0594, 0.1050	0.0413, 0.0833	0.0342, 0.0702	0.0288, 0.0675	0.0419, 0.0904
<i>R</i> ₁ , <i>wR</i> ₂ (all data)	0.0642, 0.1014	0.0564, 0.1409	0.0650, 0.0972	0.0593, 0.0880	0.1196, 0.1343	0.1332, 0.1268	0.0770, 0.0944	0.0567, 0.0783	0.0440, 0.0730	0.0580, 0.0952
Largest diff. peak and hole/e Å ⁻³	0.866, -1.186	2.479, -1.545	1.101, -0.747	0.921, -0.564	0.451, -0.543	0.564, -0.556	0.554, -0.736	0.608, -0.959	1.492, -0.672	0.912, -0.839

SHELXL-97.³¹ Refinements were generally straightforward with the following exceptions and points of note.

For **2a**, the carbon atom of the fragment of methanol in the asymmetric unit is situated at an inversion centre, which necessitates disorder of the hydroxyl group over two sites. The hydrogen atoms in this solvent moiety could not be reliably located and hence were omitted from the final least squares. The electron density map in the region of the fluorine atoms is very smeared, also due to disorder. Optimal modelling was achieved by treating each fluorine as being located over three sites. C–C and C–F bond distance restraints served to converge the model. The largest residual electron density maximum is also in this region. For **4**, the C–C and C–O distances within the diethyl ether molecule were restrained to being individually similar, and restraints were also applied to the associated atomic displacement parameters. For **7**, the fluorine disorder in the hexafluorophosphate anion was successfully modelled in a 60 : 40 ratio, whereas for **10**, the triflate anion lies proximate to an inversion centre so is disordered in a 50 : 50 ratio.

Acknowledgements

The EPSRC, the Leverhulme Trust and the Cambridge Crystallographic Data Centre are thanked for financial support.

References

- J. L. C. Rowsell and O. M. Yaghi, *Microporous Mesoporous Mater.*, 2004, **73**, 3; G. Férey, *Chem. Soc. Rev.*, 2008, **37**, 191; R. Robson, *Dalton Trans.*, 2008, 5113; S. Horike, S. Shimomura and S. Kitagawa, *Nat. Chem.*, 2009, **1**, 695; A. U. Czaja, N. Trukhan and U. Müller, *Chem. Soc. Rev.*, 2009, **38**, 1284.
- L. J. Murray, M. Dinca and J. R. Long, *Chem. Soc. Rev.*, 2009, **38**, 1294; S. Ma and H.-C. Zhou, *Chem. Commun.*, 2010, **46**, 44; X. Lin, I. Telepeni, A. J. Blake, A. Dailly, C. M. Brown, J. M. Simmons, M. Zoppi, G. S. Walker, K. M. Thomas, T. J. Mays, P. Hubberstey, N. R. Champness and M. Schröder, *J. Am. Chem. Soc.*, 2009, **131**, 2159.
- D. Dubbeldam, C. J. Galvin, K. S. Walton, D. E. Ellis and R. Q. Snurr, *J. Am. Chem. Soc.*, 2008, **130**, 10884; J. R. Li, R. J. Kuppler and H.-C. Zhou, *Chem. Soc. Rev.*, 2009, **38**, 1477; K. A. Cychoz, R. Ahmad and A. J. Matzger, *Chem. Sci.*, 2010, **1**, 293.
- J. Lee, O. K. Farha, J. Roberts, K. A. Scheidt, S. T. Nguyen and J. T. Hupp, *Chem. Soc. Rev.*, 2009, **38**, 1450; L. Ma, C. Abney and W. Lin, *Chem. Soc. Rev.*, 2009, **38**, 1248; T. Uemura, N. Yanai and S. Kitagawa, *Chem. Soc. Rev.*, 2009, **38**, 1228.
- A. C. McKinlay, R. E. Morris, P. Horcajada, G. Férey, R. Gref, P. Couvreur and C. Serre, *Angew. Chem., Int. Ed.*, 2010, **49**, 6260; A. C. McKinlay, B. Xiao, D. S. Wragg, P. S. Wheatley, I. L. Megson and R. E. Morris, *J. Am. Chem. Soc.*, 2008, **130**, 10440; W. Lin, W. J. Rieter and K. M. L. Taylor, *Angew. Chem., Int. Ed.*, 2009, **48**, 650; P. Horcajada, T. Chalati, C. Serre, B. Gillet, C. Sebrie, T. Baati, J. F. Eubank, D. Heurtaux, P. Clayette, C. Kreuz, J. S. Chang, Y. K. Hwang, V. Marsaud, P. N. Bories, L. Cynober, S. Gil, G. Férey, P. Couvreur and R. Gref, *Nat. Mater.*, 2009, **9**, 172.
- K. Uemura, R. Matsuda and S. Kitagawa, *J. Solid State Chem.*, 2005, **178**, 2420; S. M. Hawxwell, G. M. Espallargas, D. Bradshaw, M. J. Rosseinsky, T. J. Prior, A. J. Florence, J. van de Streek and L. Brammer, *Chem. Commun.*, 2007, 1532; D. Tanaka, K. Nakagawa, M. Higuchi, S. Horike, Y. Kubota, T. C. Kobayashi, M. Takata and S. Kitagawa, *Angew. Chem., Int. Ed.*, 2008, **47**, 3914; T. K. Trung, P. Trens, N. Tanchoux, S. Bourelly, P. L. Llewellyn, S. Loera-Serna, C. Serre, T. Loiseau, F. Fajula and G. Férey, *J. Am. Chem. Soc.*, 2008, **130**, 16926.
- J.-Q. Chen, Y.-P. Cai, H.-C. Fang, Z.-Y. Zhou, X.-L. Zhan, G. Zhao and Z. Zhang, *Cryst. Growth Des.*, 2009, **9**, 1605.
- C.-L. Chen, B.-S. Kang and C.-Y. Su, *Aust. J. Chem.*, 2006, **59**, 3.
- O.-S. Jung, Y. J. Kim, Y.-A. Lee, K.-M. Park and S. S. Lee, *Inorg. Chem.*, 2003, **42**, 844.

- 10 L. Raehm, L. Mimassi, C. Guyard-Duhayon, H. Amouri and M. N. Rager, *Inorg. Chem.*, 2003, **42**, 5654; B. R. Manzano, F. Jalón, M. L. Soriano, M. Carrión, M. P. Carranza, K. Mereiter, A. Rodríguez, A. de la Hoz and A. Sánchez-Migallón, *Inorg. Chem.*, 2008, **47**, 8957.
- 11 A. D. Burrows, C. G. Frost, M. F. Mahon, P. R. Raithby, C. Richardson and A. J. Stevenson, *Chem. Commun.*, 2010, **46**, 5064.
- 12 B. Ding, Y.-Y. Liu, Y.-Q. Huang, W. Shi, P. Cheng, D.-Z. Liao and S.-P. Yan, *Cryst. Growth Des.*, 2009, **9**, 593; B.-X. Dong and Q. Xu, *Cryst. Growth Des.*, 2009, **9**, 2776.
- 13 B. F. Hoskins, R. Robson and D. A. Slizys, *J. Am. Chem. Soc.*, 1997, **119**, 2952.
- 14 L. Dobrzańska, H. G. Raubenheimer and L. J. Barbour, *Chem. Commun.*, 2005, 5050.
- 15 Q. Zhao, H. Li, X. Wang and Z. Chen, *Chem. Lett.*, 2002, 988.
- 16 L. Dobrzańska, G. O. Lloyd, H. G. Raubenheimer and L. J. Barbour, *J. Am. Chem. Soc.*, 2005, **127**, 13134.
- 17 F. Meyer and H. Pritzkow, *Polyhedron*, 1999, **18**, 2769; L. L. Marques, G. M. de Oliveira, E. S. Lang, M. M. Anraku de Campos and L. R. Soccol Gris, *Inorg. Chem. Commun.*, 2007, **10**, 1083.
- 18 C.-F. Wang, Z.-Y. Zhu, Z.-X. Zhang, Z.-X. Chen and X.-G. Zhou, *CrystEngComm*, 2007, **9**, 35.
- 19 D. F. Martin, W. C. Fernelius and M. Shamma, *J. Am. Chem. Soc.*, 1959, **81**, 130.
- 20 N. S. Oxtoby, A. J. Blake, N. R. Champness and C. Wilson, *Dalton Trans.*, 2003, 3838; Z.-P. Deng, L.-N. Zhu, S. Gao, L.-H. Huo and S. W. Ng, *Cryst. Growth Des.*, 2008, **8**, 3277.
- 21 G. A. Bowmaker Effendy, K. C. Lim, B. W. Skelton, D. Sukarianingsih and A. H. White, *Inorg. Chim. Acta*, 2005, **358**, 4342; N. Schultheiss, D. R. Powell and E. Bosch, *Inorg. Chem.*, 2003, **42**, 5304.
- 22 L. Dobrzańska, G. O. Lloyd, T. Jacobs, I. Rootman, C. L. Oliver, M. W. Bredenkamp and L. J. Barbour, *J. Mol. Struct.*, 2006, **796**, 107.
- 23 Y. Gao, B. Twamley and J. M. Shreeve, *Inorg. Chem.*, 2006, **45**, 1150.
- 24 T. Jacobs, J.-A. Gertenbach, D. Das and L. J. Barbour, *Aust. J. Chem.*, 2010, **63**, 573.
- 25 X. Cui, A. N. Khlobystov, X. Chen, D. H. Marsh, A. J. Blake, W. Lewis, N. R. Champness, C. J. Roberts and M. Schröder, *Chem.–Eur. J.*, 2009, **15**, 8861.
- 26 A. Aslani and A. Morsali, *Chem. Commun.*, 2008, 3402; M. C. Bernini, F. Gándara, M. Iglesias, N. Snejko, E. Gutiérrez-Puebla, E. V. Brusau, G. E. Narda and M. A. Monge, *Chem.–Eur. J.*, 2009, **15**, 4896; J. Campo, L. R. Falvello, I. Mayoral, F. Palacio, T. Soler and M. Tomás, *J. Am. Chem. Soc.*, 2008, **130**, 2932; D. Sarma, K. V. Ramanujachary, S. E. Lofland, T. Magdaleno and S. Natarajan, *Inorg. Chem.*, 2009, **48**, 11660; P. Zhu, W. Gu, L.-Z. Zhang, X. Liu, J.-L. Tian and S.-P. Yan, *Eur. J. Inorg. Chem.*, 2008, 2971.
- 27 K. S. Min and M. P. Suh, *J. Am. Chem. Soc.*, 2000, **122**, 6834.
- 28 E. J. Cussen, J. B. Claridge, M. J. Rosseinsky and C. J. Kepert, *J. Am. Chem. Soc.*, 2002, **124**, 9574.
- 29 S. K. Ghosh, J. P. Zhang and S. Kitagawa, *Angew. Chem., Int. Ed.*, 2007, **46**, 7965.
- 30 B. Xiao, P. J. Byrne, P. S. Wheatley, D. S. Wragg, X. Zhao, A. J. Fletcher, K. M. Thomas, L. Peters, J. S. O. Evans, J. E. Warren, W. Zhou and R. E. Morris, *Nat. Chem.*, 2009, **1**, 289.
- 31 G. M. Sheldrick, *Acta Cryst. Sect. A*, 2008, **64**, 112.